

Guiding effect of quantum wells in semiconductor lasers

V.Ya. Aleshkin, N.V. Dikareva, A.A. Dubinov, B.N. Zvonkov, M.V. Karzanova, K.E. Kudryavtsev, S.M. Nekorkin, A.N. Yablonskiy

Abstract. The guiding effect of InGaAs quantum wells in GaAs- and InP-based semiconductor lasers has been studied theoretically and experimentally. The results demonstrate that such waveguides can be effectively used in laser structures with a large refractive index difference between the quantum well material and semiconductor matrix and a large number of quantum wells (e.g. in InP-based structures).

Keywords: semiconductor laser, quantum well, guiding effect.

1. Introduction

At present, an important issue is to improve the performance of semiconductor lasers: to raise their output power, quantum efficiency and beam quality [1–3]. One key component of a semiconductor laser, responsible for many of its characteristics, is its waveguide. To form a waveguide, use is commonly made of either confinement layers having a refractive index (RI) lower than that of the waveguide core (e.g. InGaP or AlGaAs layers in GaAs-based lasers) or a waveguiding layer having an RI higher (InAlGaAsP) than that of the substrate (InP). In the later case, the substrate acts as a confinement layer.

It is well known that, in the case of a symmetric waveguide (where a higher index layer is sandwiched between infinite lower index layers), TE₀ and TM₀ modes can exist at any arbitrarily small waveguide thickness [4]. Consequently, an electromagnetic mode can be confined in the vicinity of a waveguiding layer whose thickness is orders of magnitude smaller than the wavelength of the mode. In the case of semiconductor lasers operating in the 1 μm range, such a waveguiding layer can be of the order of 10 nm in thickness. Note that such thicknesses are characteristic of quantum wells acting as a gain medium in lasers. Thus, it is in principle possible to make lasers in which quantum wells play a dual role, acting as an active and a waveguiding medium. In such lasers, no conventional waveguide is needed and, hence, they have a simpler design, which is of great technological importance.

V.Ya. Aleshkin, A.A. Dubinov, K.E. Kudryavtsev, A.N. Yablonskiy
Institute for Physics of Microstructures, Russian Academy of Sciences, GSP-105, 603950 Nizhnii Novgorod, Russia;
e-mail: sanya@ipm.sci-nnov.ru;
N.V. Dikareva, B.N. Zvonkov, M.V. Karzanova, S.M. Nekorkin
Physico-Technical Research Institute, N.I. Lobachevsky Nizhnii Novgorod State University, prosp. Gagarina 23, 603950 Nizhnii Novgorod, Russia

Received 8 February 2013; revision received 27 March 2013
Kvantovaya Elektronika 43 (5) 401–406 (2013)
Translated by O.M. Tsarev

In existing semiconductor lasers, however, the waveguide is almost always asymmetric due to the specifics of the laser fabrication process – epitaxial growth of the laser and post-growth steps – because there is an interface with either air (in the case of optical pumping) or a metal (current pumping). In addition, an important role is played by the optical confinement factor, responsible for the lasing threshold. At very thin quantum wells and a small RI difference, the optical confinement factor is small (the mode is only slightly confined) and, hence, the lasing threshold is too high. A laser containing a waveguiding GaAs quantum well in a broad AlGaAs layer was demonstrated rather long ago [5]. Unfortunately, that laser had large losses because of the significant mode penetration into the heavily doped layers. Nevertheless, the guiding effect of InGaAs quantum wells has recently been used to improve the radiation pattern of high-power GaAs-based lasers [6–8].

In this paper, we describe the use of quantum wells as a waveguide and present recommendations for making lasers with such waveguides.

2. Model problem

We consider a simple model problem that describes modes in a laser with a waveguiding layer of thickness d and compare this model with a realistic model of laser containing several quantum wells. Let an electromagnetic wave propagate in the x direction and the refractive index of a semiconductor structure have the following profile:

$$n(z) = \begin{cases} n_1, & z < 0, \\ n_2, & 0 \leq z < d, \\ n_1, & d \leq z < d + L, \\ n_3, & z \geq d + L, \end{cases} \quad (1)$$

where $n_2 > n_1 \geq n_3$ and L is the transverse size of the structure.

Maxwell's equations for the $E_y(z, x)$ field of a TE mode and the $H_y(z, x)$ field of a TM mode can be written in the form

$$\frac{d^2 E_y(z, x)}{dx^2} + \frac{d^2 E_y(z, x)}{dz^2} + n^2(z) \left(\frac{k}{c}\right)^2 E_y(z, x) = 0, \quad (2)$$

$$\frac{d^2 H_y(z, x)}{dx^2} + n^2(z) \frac{d}{dz} \left[\frac{1}{n^2(z)} \frac{d^2 H_y(z, x)}{dz} \right] + n^2(z) \left(\frac{k}{c}\right)^2 H_y(z, x) = 0, \quad (3)$$

where $k = 2\pi/\lambda$; λ is the mode wavelength; and c is the speed of light in vacuum. $E_y(z, x)$, $H_y(z, x)$, $dE_y(z, x)/dz$ and $n^{-2}(z)dH_y(z, x)/dz$ are continuous across the interface between layers differing in RI. The boundary conditions for waveguide modes are $E_y(z, x)$, $H_y(z, x) \rightarrow 0$ for $z \rightarrow \pm\infty$. The solutions to Eqns (2) and (3) for the $E_y(z, x)$ and $H_y(z, x)$ fields are sought in the form

$$E_y(z, x) = \exp(ikbx) \times \begin{cases} A_1 \exp(-ikN_1z), & z < 0, \\ B_1 \exp(ikN_2z) + C_1 \exp(-ikN_2z), & 0 \leq z < d, \\ D_1 \exp(ikN_1z) + F_1 \exp(-ikN_1z), & d \leq z < d + L, \\ J_1 \exp(ikN_3z), & z \geq d + L \end{cases} \quad (4)$$

and

$$H_y(z, x) = \exp(ikbx) \times \begin{cases} A_2 \exp(-ikN_1z), & z < 0, \\ B_2 \exp(ikN_2z) + C_2 \exp(-ikN_2z), & 0 \leq z < d, \\ D_2 \exp(ikN_1z) + F_2 \exp(-ikN_1z), & d \leq z < d + L, \\ J_2 \exp(ikN_3z), & z \geq d + L, \end{cases} \quad (5)$$

where $A_1, B_1, C_1, D_1, F_1, J_1, A_2, B_2, C_2, D_2, F_2$ and J_2 are unknown constants; b is the modal index in the x direction; $N_1 = \sqrt{n_1^2 - b^2}$; $N_2 = \sqrt{n_2^2 - b^2}$; and $N_3 = \sqrt{n_3^2 - b^2}$. The dispersion relations for the TE and TM modes with unknown b then have the form

$$\frac{N_1 - N_2}{N_1 + N_2} \exp(i2kN_2d) = \frac{\exp(ikN_1L)(N_3 - N_1)(N_1 - N_2) + \exp(-ikN_1L)(N_3 + N_1)(N_1 + N_2)}{\exp(ikN_1L)(N_3 - N_1)(N_1 + N_2) + \exp(-ikN_1L)(N_3 + N_1)(N_1 - N_2)}, \quad (6)$$

$$\frac{\tilde{N}_1 - \tilde{N}_2}{\tilde{N}_1 + \tilde{N}_2} \exp(i2k\tilde{N}_2d) = \frac{\exp(ik\tilde{N}_1L)(\tilde{N}_3 - \tilde{N}_1)(\tilde{N}_1 - \tilde{N}_2) + \exp(-ik\tilde{N}_1L)(\tilde{N}_3 + \tilde{N}_1)(\tilde{N}_1 + \tilde{N}_2)}{\exp(ik\tilde{N}_1L)(\tilde{N}_3 - \tilde{N}_1)(\tilde{N}_1 + \tilde{N}_2) + \exp(-ik\tilde{N}_1L)(\tilde{N}_3 + \tilde{N}_1)(\tilde{N}_1 - \tilde{N}_2)}, \quad (7)$$

where $\tilde{N}_1 = N_1/n_1^2$; $\tilde{N}_2 = N_2/n_2^2$; and $\tilde{N}_3 = N_3/n_3^2$.

Modes are confined when d exceeds a threshold thickness, d_{th} . At $d = d_{th}$, we have $b \rightarrow n_1$ and $N_1 \rightarrow 0$, and the mode extends to $x = -\infty$. Expanding (6) and (7) in terms of the small parameter N_1 and retaining only the terms linear in N_1 , we obtain expressions for the threshold thickness d_{th} for the TE and TM modes:

$$d_{th}^{TE} = \frac{\lambda}{4\pi\sqrt{n_2^2 - n_1^2}} \times \left\{ \frac{\pi}{2} - \arctan \left[\frac{(n_2^2 - n_1^2)(1 + kL\sqrt{n_1^2 - n_3^2})^2 + n_3^2 - n_1^2}{2\sqrt{n_1^2 - n_3^2}\sqrt{n_2^2 - n_1^2}(1 + kL\sqrt{n_1^2 - n_3^2})} \right] \right\}, \quad (8)$$

$$d_{th}^{TM} = \frac{\lambda}{4\pi\sqrt{n_2^2 - n_1^2}} \times \left\{ \frac{\pi}{2} - \arctan \left[\frac{(n_2^2 - n_1^2)(n_3^2 + kLn_1^2\sqrt{n_1^2 - n_3^2})^2 + n_2^4(n_3^2 - n_1^2)}{2n_2^2\sqrt{n_1^2 - n_3^2}\sqrt{n_2^2 - n_1^2}(n_3^2 + kLn_1^2\sqrt{n_1^2 - n_3^2})} \right] \right\}. \quad (9)$$

Consider two particular structures. One of them is an $\text{In}_{0.53}\text{Ga}_{0.47}\text{As}$ layer of thickness d grown on an InP substrate and buried under an InP layer of thickness L . At $\lambda = 1.55 \mu\text{m}$, we have $n_1(\text{InP}) = 3.17$ [9], $n_2(\text{In}_{0.53}\text{Ga}_{0.47}\text{As}) = 3.6$ [10] and $n_3(\text{vacuum}) = 1$. The other structure is an $\text{In}_{0.2}\text{Ga}_{0.8}\text{As}$ layer of thickness d grown on a GaAs substrate and buried under a GaAs layer of thickness L . In this case, at $\lambda = 1 \mu\text{m}$ we have $n_1(\text{GaAs}) = 3.51$ [11], $n_2(\text{In}_{0.2}\text{Ga}_{0.8}\text{As}) = 3.56$ (approximation from Refs [11, 12]) and $n_3(\text{vacuum}) = 1$. Figure 1 shows the threshold thickness d_{th} as a function of L for the TE and TM modes in the two structures. It is seen that InP/ $\text{In}_{0.53}\text{Ga}_{0.47}\text{As}$ /InP structures with quantum well thicknesses under 10 nm have confined TE and TM modes at L above 2 and 3 μm , respectively. GaAs/ $\text{In}_{0.2}\text{Ga}_{0.8}\text{As}$ /GaAs structures with $L > 2.5 \mu\text{m}$ have confined TE and TM modes when d exceeds 30 nm. Therefore, confined modes in such a structure are possible when it contains several quantum wells less than 10 nm in thickness.

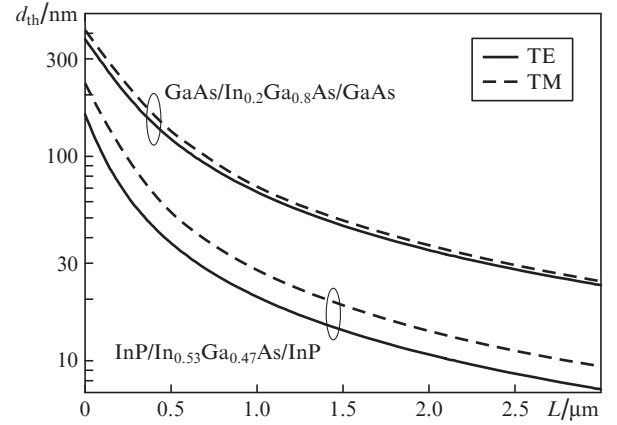


Figure 1. Threshold thickness d_{th} as a function of L for the TE and TM modes in an InP/ $\text{In}_{0.53}\text{Ga}_{0.47}\text{As}$ /InP structure at a wavelength of 1.55 μm and in a GaAs/ $\text{In}_{0.2}\text{Ga}_{0.8}\text{As}$ /GaAs structure at a wavelength of 1 μm (293 K).

Consider in this model the behaviour of the modal index for waveguiding quantum wells. Let $kN_2d \ll 1$, $b \rightarrow n_1$ and $N_1 \rightarrow 0$. This means that $d \ll 75 \text{ nm}$ and $L \gg 0.2 \mu\text{m}$ for the InP/ $\text{In}_{0.53}\text{Ga}_{0.47}\text{As}$ /InP structure and $d \ll 134 \text{ nm}$ and $L \gg 0.45 \mu\text{m}$ for the GaAs/ $\text{In}_{0.2}\text{Ga}_{0.8}\text{As}$ /GaAs structure. Then, expanding (6) and (7) in terms of the small parameters N_1 and d , we obtain for the TE and TM modes, respectively,

$$\exp(-2k\sqrt{b^2 - n_1^2}L) + 2\sqrt{b^2 - n_1^2}[kd(n_2^2 - n_1^2)]^{-1} = 1, \quad (10)$$

$$\exp(-2k\sqrt{b^2 - n_1^2}L) + 2\sqrt{b^2 - n_1^2}n_2^2[kd(n_2^2 - n_1^2)n_1^2]^{-1} = 1. \quad (11)$$

The solutions to these equations have the form

$$b^{TE} = \left\{ n_1^2 + \left[\frac{k}{2}d(n_2^2 - n_1^2) + \frac{1}{2kL}W(-s\exp(-s)) \right]^2 \right\}^{1/2}, \quad (12)$$

$$b^{TM} = \left\{ n_1^2 + \left[\frac{k}{2}\frac{n_1^2}{n_2^2}d(n_2^2 - n_1^2) + \frac{1}{2kL}W\left(-\frac{n_1^2}{n_2^2}s\exp\left(-\frac{n_1^2}{n_2^2}s\right)\right) \right]^2 \right\}^{1/2}, \quad (13)$$

where $s = k^2 d L (n_2^2 - n_1^2)$ and $W(x)$ is the Lambert W -function [13].

Let us calculate the optical confinement factor for the TE and TM modes in the waveguiding structures under consideration (the waveguiding and active layers are taken to be identical in thickness):

$$\Gamma_{\text{TE,TM}} = \left[\int_0^d |E_{y,z}(z,x)|^2 dz \right] \left[\int_{-\infty}^{\infty} |E_{y,z}(z,x)|^2 dz \right]^{-1}, \quad (14)$$

where $E_z(z,x) = -bH_y(z,x)/n^2(z)$. At larger optical confinement factors, smaller gain coefficients are needed for the onset of lasing. Figure 2 shows the optical confinement factor as a function of waveguiding layer thickness d for the TE and TM modes in the InP/In_{0.53}Ga_{0.47}As/InP (a) and GaAs/In_{0.2}Ga_{0.8}As/GaAs (b) structures at different values of L . Also shown for comparison are the optical confinement factors of conventional waveguides. It is seen in Fig. 2b that the optical confinement factor of the GaAs/In_{0.2}Ga_{0.8}As/GaAs structure is about one order of magnitude smaller than that of a conventional waveguide with InGaP confinement layers. At the

same time, at active layer thicknesses above 60 nm the optical confinement factor of the InP/In_{0.53}Ga_{0.47}As/InP structure (Fig. 2a) approaches the Γ of a conventional InP/InGaAsP/InP waveguide. This means that the fundamental mode in the conventional waveguide is confined on a length scale smaller than the waveguide thickness. Consequently, an InP/In_{0.53}Ga_{0.47}As/InP heterostructure laser having six 10-nm-thick quantum wells will have the same optical confinement factor as a laser with a thick InGaAsP waveguiding layer, so this layer is unnecessary.

Note that the distinction between the behaviours of the optical confinement factors of the GaAs/In_{0.2}Ga_{0.8}As/GaAs and InP/In_{0.53}Ga_{0.47}As/InP structures arises from the marked difference between n_1 and n_2 : $n_1 = 3.51$ and $n_2 = 3.56$ in the former structure and $n_1 = 3.17$ and $n_2 = 3.6$ in the latter.

3. Realistic model

In contrast to the model problem considered above, let us discuss a realistic model for a laser with a gain medium (of thickness $d = p d_{\text{QW}}$) consisting of several identical quantum wells ($p = 1-6$) of thickness $d_{\text{QW}} = 10$ nm separated by barriers 20 (in the InP/In_{0.53}Ga_{0.47}As/InP structure) and 100 nm (in the GaAs/In_{0.2}Ga_{0.8}As/GaAs structure) thick. For a current-pumped laser, we take into account contact with a metal and doping of the substrate (donor concentration of $2 \times 10^{18} \text{ cm}^{-3}$) and contact layer (acceptor concentration of $2 \times 10^{18} \text{ cm}^{-3}$). Note that, in this case, doping of the substrate and contact layer also ensures a guiding effect for the TE and TM modes because it slightly reduces the RI of the semiconductor. Such waveguides, however, have appreciable losses because of the field penetration into the doped regions and light absorption by free carriers. Such waveguides were used in the first diode lasers with a p-n homojunction [3]. The influence of this effect is stronger at smaller $n_2 - n_1$ and $n_2 - n_3$ differences and lower values of d and p . Moreover, in the case of the TM mode a guiding effect may result from surface plasma wave excitation in the laser at the semiconductor-metal interface [14]. In the near-IR spectral region, however, such a wave will have large losses, so this situation is here left out of consideration.

The electric field distribution, propagation constants and optical confinement factors of modes were determined numerically from Eqns (2), (3) and (14) using the transfer matrix method for both cases and both structures. The doping effect on the RI of the semiconductor was taken into account as [15]

$$n_d = \left(n^2 - \frac{4\pi e^2 N_d}{m^* \omega^2} \right)^{1/2}, \quad (15)$$

where n_d and n are the refractive indices of the doped and undoped semiconductor, respectively; e is the electronic charge; N_d is the carrier concentration; ω is frequency; and m^* is the carrier effective mass, taken from Ref. [11].

Figure 3 shows the optical confinement factor as a function of gain medium thickness (number of quantum wells) for the TE and TM modes and different L values in the InP/In_{0.53}Ga_{0.47}As/InP structure. It is seen that the presence of barriers between quantum wells in the gain medium of the laser has little effect on the optical confinement factor. The exact solution indicates that there is a threshold for the existence of TE and TM modes in this structure with $L = 1 \mu\text{m}$. The threshold for the TM mode is higher (three quantum wells)

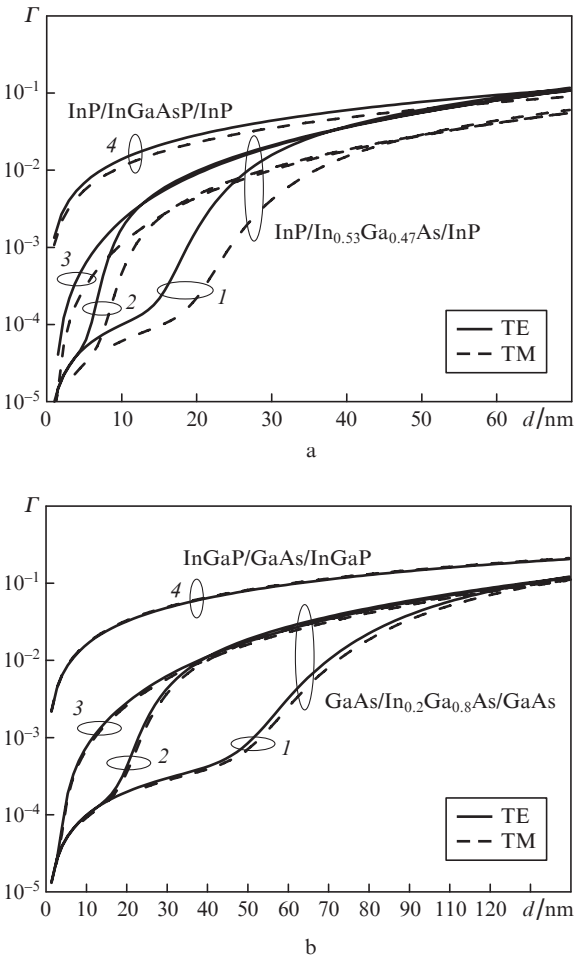


Figure 2. Optical confinement factor as a function of active waveguiding layer thickness d for the TE and TM modes (a) in an InP/In_{0.53}Ga_{0.47}As/InP structure at a wavelength of 1.55 μm and (b) in a GaAs/In_{0.2}Ga_{0.8}As/GaAs structure at a wavelength of 1 μm : $L = (1)$ 1, (2) 3 and (3) 20 μm . Curves (4) represent the optical confinement factor as a function of active layer thickness for the TE and TM modes (a) in a conventional InP/InGaAsP/InP waveguide having a 1- μm InGaAsP layer and (b) in a InGaP/GaAs/InGaP waveguide having a 1- μm GaAs layer.

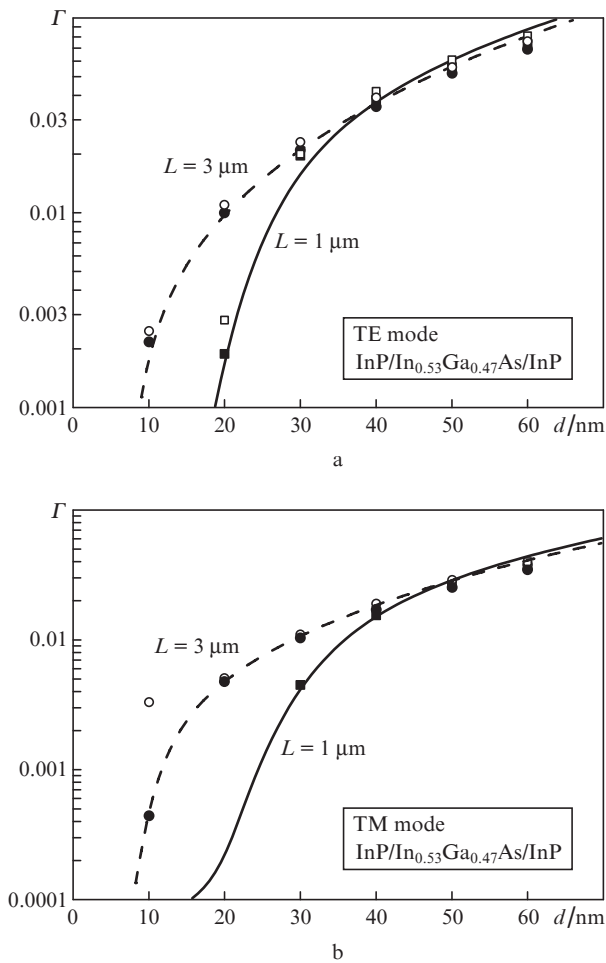


Figure 3. Optical confinement factor calculated as a function of active waveguiding layer thickness d by Eqn (14) for the (a) TE and (b) TM modes in $\text{InP}/\text{In}_{0.53}\text{Ga}_{0.47}\text{As}/\text{InP}$ structures with $L = 1$ and $3 \mu\text{m}$ at a wavelength of $1.55 \mu\text{m}$. The filled squares and circles represent the optical confinement factors calculated exactly for the TE and TM modes of a gain medium consisting of p quantum wells of thickness $d_{\text{QW}} = 10 \text{ nm}$ ($d = pd_{\text{QW}}$) separated by 20-nm-thick barriers. The open squares and circles represent the optical confinement factors for the TE and TM modes of the same quantum wells with allowance for doping and $n_3 = 0.5 + 10i$ [16].

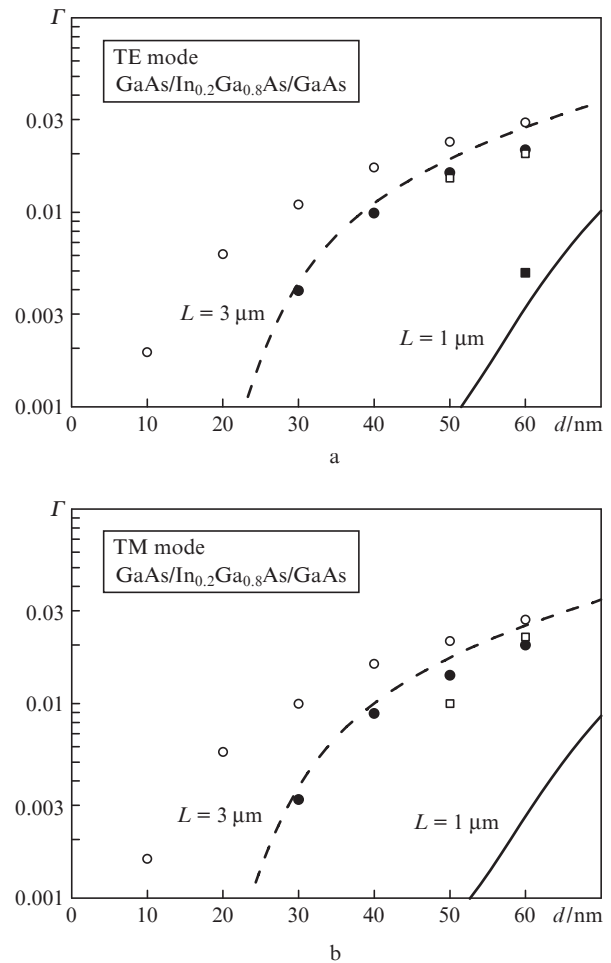


Figure 4. Optical confinement factor calculated as a function of active waveguiding layer thickness d by Eqn (14) for the (a) TE and (b) TM modes in $\text{GaAs}/\text{In}_{0.2}\text{Ga}_{0.8}\text{As}/\text{GaAs}$ structures with $L = 1$ and $3 \mu\text{m}$ at a wavelength of $1 \mu\text{m}$. The filled squares and circles represent the optical confinement factors calculated exactly for the TE and TM modes of a gain medium consisting of p quantum wells of thickness $d_{\text{QW}} = 10 \text{ nm}$ ($d = pd_{\text{QW}}$) separated by 100-nm-thick barriers. The open squares and circles represent the optical confinement factors for the TE and TM modes of the same quantum wells with allowance for doping and $n_3 = 0.25 + 7i$ [16].

than that for the TE mode (two quantum wells). Structure–metal contact and doping of the substrate and contact layer influence the TE mode only at a small number of quantum wells (one or two) and small L . In contrast, structure–metal contact has a strong effect on the TM mode at small L . As a result, the TM mode for the structure with $L = 1 \mu\text{m}$ exists only in a gain medium consisting of more than five quantum wells.

Figure 4 shows analogous dependences of the optical confinement factor for the $\text{GaAs}/\text{In}_{0.2}\text{Ga}_{0.8}\text{As}/\text{GaAs}$ structure. It is seen that, in contrast to the $\text{InP}/\text{In}_{0.53}\text{Ga}_{0.47}\text{As}/\text{InP}$ structure, taking into account the barriers between the quantum wells in the gain medium of the laser has a significant effect on the optical confinement factor and the threshold for the existence of confined modes. At $L = 1 \mu\text{m}$, the threshold for the TE mode is six 10-nm-thick quantum wells and that for the TM mode is above seven quantum wells. At $L = 3 \mu\text{m}$, the threshold for both the TE and TM modes is three 10-nm-thick quantum wells. The structure–metal contact and doping

of the substrate and contact layer have a crucial effect on the optical confinement factor at small p and L . Mode confinement in such a structure is mainly due to doping of the substrate and contact layer, which causes considerable losses through free carriers despite the larger optical confinement factor in comparison with the undoped structure. At $L = 1 \mu\text{m}$, the threshold for both the TE and TM modes is five 10-nm-thick quantum wells. It is for this reason that a more complex waveguide design compared to that considered by us was used by Pietrzak et al. [6, 7] for making high-power GaAs-based lasers. To increase the index difference between the quantum wells and the semiconductor matrix around them, a lightly doped $\text{Al}_{0.1}\text{Ga}_{0.9}\text{As}$ layer about 10- μm thick, with an RI considerably smaller than that of GaAs, was used as a matrix. Moreover, for wave confinement in the $\text{Al}_{0.1}\text{Ga}_{0.9}\text{As}$ layer, it was sandwiched between extra $\text{Al}_{0.2}\text{Ga}_{0.8}\text{As}$ layers $\sim 1 \mu\text{m}$ thick. Note that the design proposed in this study can be effectively used for InP-based lasers.

4. Experimental

For experimental studies of the guiding effect of InGaAs quantum wells in InP-based lasers, structure 1, containing three quantum wells (Table 1) and intended for optical pumping, and structure 2, containing four quantum wells (Table 2) and intended for current pumping, were grown by atmospheric pressure metalorganic vapour phase epitaxy in a horizontal reactor. After thinning, structure 1 was cleaved into thin strips 1 mm in width. Structure 2 was used to produce a 1-mm-long laser diode with a 100- μm -wide active region by chemically etching the contact layer beyond the active stripe, followed by proton implantation into the stripped InP surface. After cleaving, the chip was soldered, with the structure down, onto a copper heat sink. In both cases, cleaved (110) facets were used as laser mirrors.

Table 1. Parameters of the layers in laser structure 1.

No.	Function	Doping and composition	Thickness/nm
1	Substrate	n ⁺ -InP	–
2	Waveguiding	n-InP	1862
3	QW 1	In _{0.53} Ga _{0.47} As	9
4	Waveguiding	i-InP	49
5	QW 2	In _{0.53} Ga _{0.47} As	9
6	Waveguiding	i-InP	49
7	QW 3	In _{0.53} Ga _{0.47} As	9
8	Waveguiding	i-InP	49
9	Waveguiding	p-InP	1274

Table 2. Parameters of the layers in laser structure 2.

No.	Function	Doping and composition	Thickness/nm
1	Substrate	n ⁺ -InP	–
2	Waveguiding	n-InP	368
3	QW 1	In _{0.65} Ga _{0.35} As	12
4	Waveguiding	i-InP	92
5	QW 2	In _{0.65} Ga _{0.35} As	12
6	Waveguiding	i-InP	92
7	QW 3	In _{0.65} Ga _{0.35} As	12
8	Waveguiding	i-InP	92
9	QW 4	In _{0.65} Ga _{0.35} As	12
10	Waveguiding	i-InP	92
11	Waveguiding	p-InP	2208
12	Contact	p ⁺ -In _{0.53} Ga _{0.47} As	184

The lasing threshold of structure 1 at liquid-nitrogen temperature was reached (Fig. 5) at a frequency-doubled (532 nm) cw Nd:YAG pump power density of $\sim 260 \text{ W cm}^{-2}$, which points to effectiveness of the guiding effect of InGaAs quantum wells in InP-based lasers. Note that laser emission was only observed on the cleaved facet of the structure, which indicated that scattering in the waveguide was extremely weak and that it had good directivity properties. The room-temperature lasing threshold was substantially higher ($\sim 5 \text{ kW cm}^{-2}$ under pumping with a Spectra-Physics MOPO-SL parametric oscillator at a wavelength of 530 nm, pulse duration of $\sim 10 \text{ ns}$ and pulse repetition rate of 10 Hz). The light was detected by a linear photodiode array (working range 0.62–2.2 μm). As shown by Thijs et al. [17], this large difference between the 77- and 293-K lasing thresholds is due to the considerable increase in Auger recombination frequency with increasing

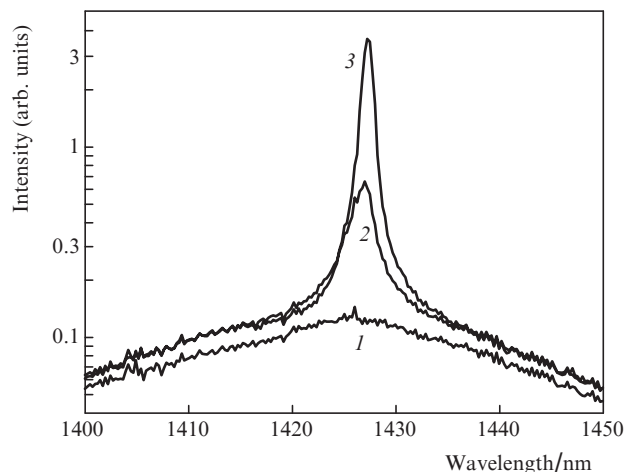


Figure 5. 77-K lasing spectra of a three quantum well InP/In_{0.53}Ga_{0.47}As structure at frequency-doubled (532 nm) cw Nd:YAG pump power densities of (1) 250, (2) 260 and (3) 315 W cm^{-2} .

temperature in In_{0.53}Ga_{0.47}As quantum wells lattice-matched to InP. According to their findings, the use of strained quantum wells can substantially reduce the room-temperature lasing threshold. In view of this, structure 2 was grown with strained In_{0.65}Ga_{0.35}As quantum wells, but their thickness (Table 2) considerably exceeded the intended one (7 nm) and approached the critical thickness, which probably had an adverse effect on the quality of the structure. Moreover, the In_{0.53}Ga_{0.47}As contact layer was rather thick, which strongly increased the loss in the laser. As a result, the lasing threshold was too high, 10 A at 77 K, and the emission wavelength changed to 1.55 μm . We measured the radiation pattern of the laser in a plane normal to the p–n junction (Fig. 6). The radiation pattern was found to agree well with that calculated as described elsewhere [3], lending further support to our theoretical conclusions as to the effectiveness of using modes confined near quantum wells in lasers with a large index difference between the quantum well material and surrounding semiconductor.

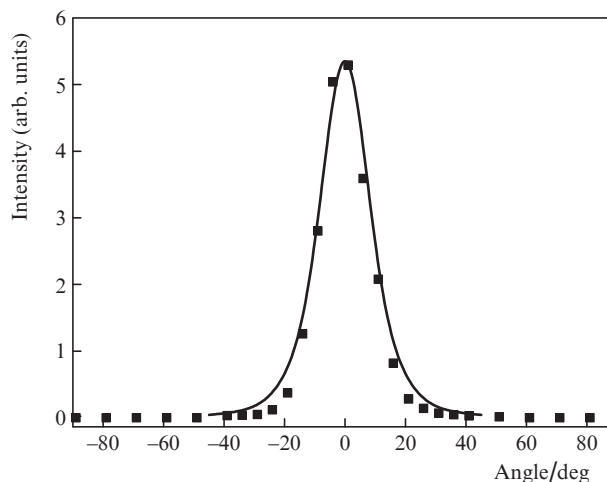


Figure 6. 77-K angular radiation pattern of laser structure 2 in a plane normal to the p–n junction. The filled squares represent the experimental data and the solid line is a theoretical fit.

5. Conclusions

It is worth noting the advantages and drawbacks of quantum well waveguide structures. Clearly, in contrast to lasers with broad waveguides, they possess excellent mode selectivity. In particular, the laser waveguide designs under discussion support only one mode. Moreover, they offer extremely weak laser radiation scattering. Yet another obvious advantage is the simplified laser design. One of their drawbacks is the increased light absorption by free carriers – the cost of the broad mode confinement region. This problem can, however, be obviated by using a special doping profile. In our laser design, charge carriers are not confined by wide-band-gap layers in the waveguiding region, so carriers that are not captured at the quantum wells can diffuse into the p- and n-regions. Another drawback is that such waveguides can only be used in semiconductor systems having a sufficient refractive index difference between the quantum wells and surrounding material.

Acknowledgements. This work was supported by the Dynasty Foundation, the RF President's Grants Council (Support to Young Russian Scientists Programme, Grant No. MK-678.2012.2; Support to the Leading Scientific Schools Programme, Grant No. NSh-4756.2012.2), the RF Ministry of Education and Science (federal targeted programme The Scientists and Science Educators of Innovative Russia, 2009–2013, State Contract No. 8578), the Physical Sciences Division of the Russian Academy of Sciences (basic research programme No. 7), the Russian Foundation for Basic Research (RFBR) (Grant No. 13-02-97062-r_povolzh'e) and the Belarusian Republican Foundation for Fundamental Research (BRFFR) (RFBR–BRFFR joint research agreement, Grant No. 12-02-90024-Bel).

References

1. Bachmann F., Loosen P., Poprawe R. *High Power Diode Laser. Technology and Applications* (Berlin: Springer, 2007).
2. Zhukov A.E. *Lazery na osnove poluprovodnikovoykh nanostruktur* (Semiconductor Nanostructure Lasers) (St. Petersburg: Elmor, 2007).
3. Casey H.C., Panish M.B. *Heterostructure Lasers* (New York: Academic, 1978).
4. Yariv A., Yeh P. *Optical Waves in Crystals* (New York: John Wiley & Sons, Inc., 1984).
5. Dupuis R.D., Dapkus P.D., Chin R., Holonyak N. Jr., Kirchoefer S.W. *Appl. Phys. Lett.*, **34**, 265 (1979).
6. Pietrzak A., Wenzel H., Erbert G., Tränkle G. *Opt. Lett.*, **33**, 2188 (2008).
7. Pietrzak A., Crump P., Wenzel H., Erbert G., Bugge F., Tränkle G. *IEEE J. Sel. Top. Quantum Electron.*, **17**, 1715 (2011).
8. Slipchenko S.I., Podoskin A.A., Pikhtin N.A., Leshko A.Yu., Rozhkov A.V., Tarasov I.S. *Pis'ma Zh. Tekh. Fiz.*, **39** (8), 9 (2013).
9. Martin P., El Skouri M., Chusseau L., Alibert C., Bissessur H. *Appl. Phys. Lett.*, **67**, 881 (1995).
10. Pan J.-W., Shieh J.-L., Gau J.-H., Chyi J.-I., Lee J.-C., Ling K.-J. *J. Appl. Phys.*, **78**, 442 (1995).
11. Madelung O. *Semiconductors: Data Handbook* (New York: Springer-Verlag, 2003).
12. Reentila O., Mattila M., Sopanen M., Lipsanen H. *J. Appl. Phys.*, **101**, 033533 (2007).
13. Corless R.M., Gonnet G.H., Hare D.E.G., Jeffrey D.J., Knuth D.E. *Adv. Comput. Math.*, **5**, 329 (1996).
14. Tredicucci A., Gmachl C., Capasso F., Hutchinson A.L., Sivco D.L., Cho A.Y. *Appl. Phys. Lett.*, **76**, 2164 (2000).
15. Zavada J.M., Weiss B.L., Bradley I.V., Theys B., Chevallier J., Rahbi R., Addinall R., Newman R.C., Jenkinson H.A. *J. Appl. Phys.*, **71**, 4151 (1992).
16. Palik E.D. *Handbook of Optical Constants of Solids* (New York: Acad. Press, 1998).
17. Thijs P.J.A., Tiemeijer L.F., Binsma J.J.M., van Dongen T. *IEEE J. Quantum Electron.*, **30**, 477 (1994).